2

Conf-900926--6

UCRL- JC-104217
PREPRINT

Received by OSTI
JAN 28 1991

Advances in Time-Dependent Methods for Multiphoton Processes

Kenneth C. Kulander, Kenneth J. Schafer and Jeffrey L. Krause
Lawrence Livermore National Laboratory
P. O. Box 808
Livermore, California 94550

This paper was prepared for submittal to
International Conference on Multiphoton Processes
Paris, France
September 24-29, 1990

September 1990

Lawrence Livermore National Laboratory

This is a preprint of a paper intended for publication in a journal or proceedings. Since changes may be made before publication, this preprint is made available with the understanding that it will not be cited or reproduced without the permission of the author.

DISTRIBUTION OF THIS DOCUMENT IS UNLIMITED

DISCLAIMER

This document was prepared as an account of work sponsored by an agency of the United States Government. Neither the United States Government nor the University of California nor any of their employees, makes any warranty, express or implied, or assumes any legal liability or responsibility for the accuracy, completeness, or usefulness of any information, apparatus, product, or process disclosed, or represents that its use would not infringe privately owned rights. Reference herein to any specific commercial products, process, or service by trade name, trademark, manufacturer, or otherwise, does not necessarily constitute or imply its endorsement, recommendation, or favoring by the United States Government or the University of California. The views and opinions of authors expressed herein do not necessarily state or reflect those of the United States Government or the University of California, and shall not be used for advertising or product endorsement purposes.

UCRL-JC--104217

DE91 006712

ADVANCES IN TIME-DEPENDENT METHODS FOR MULTIPHOTON PROCESSES

Kenneth C. Kulander, Kenneth J. Schafer and Jeffrey L. Krause
V- and H-Divisions, Physics Department
Lawrence Livermore National Laboratory
Livermore, California 94550

ABSTRACT

This paper discusses recent theoretical results on above threshold ionization, harmonic generation and high-frequency, high intensity suppression of ionization. These studies of multiphoton processes in atoms and molecules for short, intense pulsed optical lasers have been carried out using techniques which involve the explicit solution of the time-dependent Schrödinger equation.

INTRODUCTION

In the past few years several developments in the use of time-dependent methods for studying laser-atom interactions in intense, short pulsed laser fields have occured. The important advances include the calculation of above threshold ionization spectra for realistic (three-dimensional) atomic systems, the calculation of photon emission from laser excited atoms and some recent results on high frequency, high intensity suppression of ionization. For intensities within the regime in which perturbative techniques are valid up to 10^{15} - 10^{16} W/cm^2, time-dependent techniques have provided accurate results for the measured photoelectron energy and angular distributions and for photon emission for many atomic species. Most of these results have been obtained from single-electron calculations which are exact for hydrogenic systems, but only approximate for the multi-electron systems considered. For the hydrogen atom, similarly comprehensive results have been obtained using Floquet methods.[1] At even higher intensities, multi-electron processes may become important, meaning the calculations in this regime will be significantly more complicated. The intensity for which this is true depends on wavelength, target species and pulse length.

Time dependent methods have also been employed using one-dimensional model potentials to study multiphoton processes through "numerical experiments." Much insight has been gained from these calculations, which recently have been reviewed extensively by Eberly, et al.[2] and therefore will not be discussed further here except in connection with the stabilization results.

DISTRIBUTION OF THIS DOCUMENT IS UNLIMITED

MASTER

In the next section we briefly discuss the new techniques being used to study intense field, multiphoton phenomena. The following section includes illustrative results for photoelectron spectra. In the fourth section we discuss the calculation of the single atom photoemission spectrum including harmonic generation. The final section provides a discussion of a systematic investigation of ionization suppression in an intense high-frequency field.

METHOD

The time-dependent Schrödinger equation is solved using a finite difference representation for the electronic wave function. In our earlier work[3] we employed cylindrical coordinates, ρ, z and φ, to represent the time-dependent electronic wave function. Recently, we have developed codes which use a spherical coordinate system, r, θ and φ.[4] We consider only the case of linear polarization, so that the azimuthal quantum number is conserved. Therefore the equations involve only the two important spatial dimensions. This is true even in the cases of the multi-electron systems we have studied because of the form of the model potentials we have employed to approximate the effects of the other atomic electrons not explicitly included in the calculations.[5] The change to spherical coordinates has allowed us to (1) utilize a more compact description (fewer grid points) of the wave function, (2) reduce the storage requirements and increase the speed of the calculation (3) easily obtain angular distributions and excited state probability amplitudes for the electronic wave function after (or during) the laser pulse and (4) use ℓ-dependent effective potentials.[4,6] The time integration still can be carried out using an alternating-directions, implicit (Peaceman-Rachford) method.[7]

Because the relevant Schrödinger equation is solved explicitly, the intra-atomic interactions are treated on an equal footing with the laser-electron interaction, i.e., no assumptions are made about the relative strengths of these interactions. Also, by obtaining a solution of the time-dependent problem, the dependence of the results on the pulse shape can be investigated.

We expand our time-dependent wave function in spherical harmonics,

$$\psi(r,\theta,\varphi) = \Sigma_{\ell m}\, \chi_{\ell m}(r)\, Y_{\ell m}(\theta,\varphi)/r \qquad (1)$$

Inserting this expansion in the time-dependent Schrödinger equation, we obtain the following equation for the orbital

$$i\frac{\partial}{\partial t}\chi_{\ell m}(r) = \Sigma_{\ell'}(H_r + H_{\ell\ell'})\chi_{\ell' m}(r) \qquad (2)$$

where

$$H_r = T_r + V_r \tag{3}$$

and

$$H_{\ell\ell'} = V_I \tag{4}$$

As previously, we assume the laser is polarized in the z-direction and is sufficiently intense to be treated classically. Thus,

$$V_I = - e\, z\, f(t)\, E_{max} \sin(\omega t) \tag{5}$$

which couples ℓ' to $\ell \pm 1$. The envelope function, f(t), increases to unity at the peak of the pulse. The discretized equations are derived variationally from the equivalent Lagrangian formulation, explicitly taking into account the r=0 boundary. Using a three-point second difference for the radial kinetic energy, T_r, both parts of the Hamiltonian are tridiagonal. Therefore, we can use the Peaceman-Rachford time propagator,

$$\psi^{n+1} = [1+i\tau H_r]^{-1}[1+i\tau V_I]^{-1}[1-i\tau V_I][1-i\tau H_r]\psi^n \tag{6}$$

where $\tau = \Delta t/2$ and ψ^n is a vector containing the values of the wave function at the grid points at the time $t = n\Delta t$. This propagator is accurate through second order in the time-step and, since it involves only tridiagonal matrices, can be efficiently and rapidly inverted with vectorizable operations.

Similar integration schemes have been employed by other workers in this field to explicitly integrate the time-dependent Schrödinger equation. Hermann and Fleck[8] used this coordinate system but employed fast Fourier transforms to evaluate the kinetic energy with a split-operator propagator. DeVries[9] also used spherical coordinates and finite difference spatial derivatives combined with a different split-operator propagator. LaGattuta[10,11] has used a fourth-order predictor-corrector to evolve hydrogenic wave functions on a grid in spherical coordinates. Finally, various basis expansions have been developed to represent the time-dependent wave function. Pindzola and coworkers[12,13] and Tang, et al.[14] have used a spline basis, Laikos and Horbatsch[15] have used a gaussian function and Collins and Mertz[16] have expanded the wave function in terms of Volkov functions. In all these basis expansion approaches, a system of first order temporal equations is solved. In contrast to

these methods, Faisal and Moloney[17] developed a formalism to study multiphoton ionization using a non-Hermitian Schrödinger equation.

Many properties of interest can be obtained from the time-dependent wave function either during or after the laser pulse. Induced photoemission rates are calculated from the time-dependent dipole of the excited system.[18] This technique has been used by several researchers to obtain harmonic emission rates which will be discussed below. The energy and angular distributions of emitted electrons can be calculated by projecting the final wave function onto field-free (scattering) eigenstates of the system.[2,11] This requires the generation of these states, then the calculation of the overlap between the wave function and this continuum of states. Similarly, transition probabilities to excited states can be determined. We have developed a significantly more efficient method for evaluating these distributions.[4,6] Because our wave function is time-dependent, it contains results for all possible energies of the electron. Using an energy "window" operator, we can easily determine the total probability in the final wave function of the energy of the electron falling in a narrow range (window) about a particular chosen energy. If the window is narrower than any significant structure in the energy distribution, we can efficiently map out the electron energy distributions by performing this analysis at a series of energies separated by the width of the window. By preceding this analysis with projections onto the spherical harmonics, which is trivial when using a spherical coordinate system, we can also obtain the angular distributions.

To be more explicit, we define the operator

$$W(E_i,n,\gamma) = \gamma^{2^n}/((H_o - E_i)^{2^n} + \gamma^{2^n}). \tag{7}$$

H_o is the field-free atomic Hamiltonian. Then the probability within $\pm\gamma$ of the energy E_i is given by

$$P(E_i,n,\gamma) = \langle\psi_f|W(E_i,n,\gamma)|\psi_f\rangle. \tag{8}$$

This can be evaluated very easily because the operator can be expressed as a product of operators of the form $\gamma/(H_o - E_i \pm i\gamma)$ operating on a known function which, for a discretized representation of the Hamiltonian, can by inverted very efficiently. In this way we determine the energy and angular distributions of the emitted electrons along with the probabilities of populating excited bound states by the pulse.

This summarizes the techniques currently being used. In the following sections we present some recent results including electron and photon emission and for suppression of

ionization at high frequency and high intensity.

ABOVE THRESHOLD IONIZATION

Recently a number of theoretical studies of photoelectron energy distributions have been carried out for realistic (three dimensional) atomic systems. Most of the effort has focused on hydrogen for which it is possible to perform exact calculations. Chu and Cooper[19], Crance[20] and Potvliege and Shakeshaft[21,22] have used Floquet methods to calculate ATI spectra at intensities in the non-perturbative regime. Spectra for hydrogen were also obtained by LaGattuta[11] who projected a time-dependent wave function onto Coulomb continuum states. Using our method described above, we have obtained energy and angular distributions for a number of wavelengths, intensities and pulse shapes for both hydrogen and xenon. A representative result of our energy analysis for a trapezoidal pulse which rises linearly over two optical cycles, is constant at 2×10^{13} W/cm^2 for 10 cycles then is ramped linearly down over a final two cycles is shown in figure 1. The photon energy is 2.33 eV

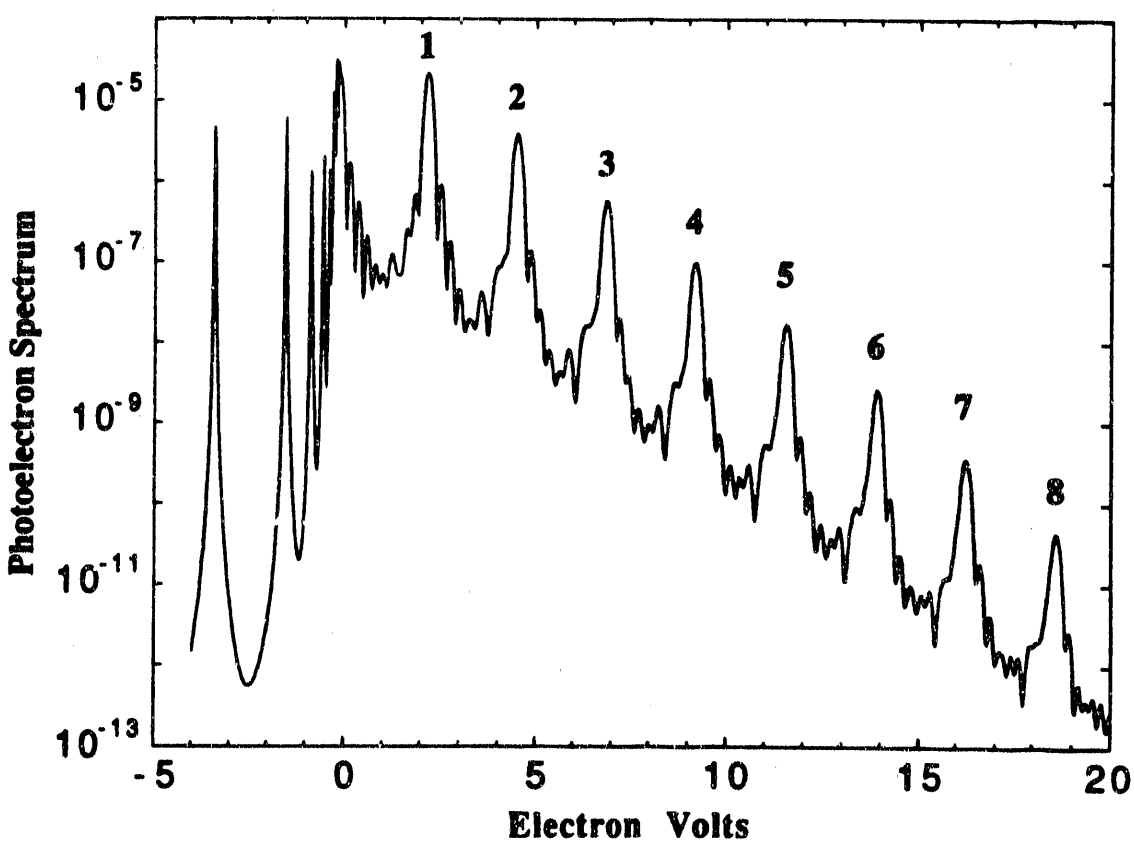

Figure 1-Hydrogen ATI spectrum at 532 nm and 2×10^{13}W/cm^2

(532 nm). The peaks for E < 0 correspond to population remaining in bound excited states at the end of the pulse. The ATI peaks are denoted by s, the number of excess photons which have been absorbed by the escaping electron. The expected energy of the electron emitted at the intensity I in peak s is given by

$$E_s(I) = (n+s)\hbar\omega - I_o - E_p(I) \qquad (9)$$

where I_o is the field-free ionization potential, E_p is the ponderomotive shift given by $I/4\omega^2$ in atomic units and n is the minimum number of photons required to ionize the atom. At this intensity the ponderomotive shift of the ionization potential has caused the lowest peak (s=0) to fall within the high Rydberg states. As discussed by many authors,[23-27] the shift of the peaks due to the ponderomotive potential can only be observed experimentally with pulse lengths short compared to the time it takes the emitted electron to exit the focal volume.

The ATI peaks appear exactly at the shifted energies given by equation (9) and are separated by one photon energy. The widths and shapes of these calculated ATI peaks are consistent with the Fourier transform of the pulse shape, as would be expected if no resonance enhancements are involved. Since the rise and fall of the pulse is very rapid, the system spends little time on resonance so that their effects are not seen in this energy distribution. The ionization rate for the separate peaks are obtained by integrating the probability under the peak and dividing by the time interval for the flat (constant intensity) part of the pulse. The rates for the lowest ATI peak agree well with the Floquet results of Potvliege and Shakeshaft.[22] They are not able to obtain results for the higher peaks using their current method.

The influence of intermediate resonances can be seen in the spectra shown in figure 2, which compares a trapezoidal pulse to a $\sin^2$ pulse at 5×10^{13} W/cm^2. Structure in each ATI peak correspond to excited states which are Stark shifted into resonance during the rise and fall of the pulse.[24-27] The photoelectron is then produced with a ponderomotive shift particular to that resonant intensity as given by equation (9).

PHOTOEMISSION/HARMONIC GENERATION

Atoms being excited by a strong laser field can generate a significant amount of radiation, particularly at frequencies which are odd multiples of the pump frequency. Recent experiments[28,29] have shown that very strong, very high-order harmonics can be produced provided the gas density is high. This is because harmonic conversion is a coherent process and therefore the output is proportional to the square of the gas density. Up to the thirty-third harmonic of Nd:YAG has been produced in argon.[30] Wave lengths as short as 15nm have been reported[28] using a KrF (248nm) pump and neon as the medium.

The theory of harmonic generation has two parts.[31-33] First, the spectrum emitted by the individual atoms must be calculated for a range of pump intensities in order to take into account the spatial distribution of intensities in the focal volume. The calculated harmonic

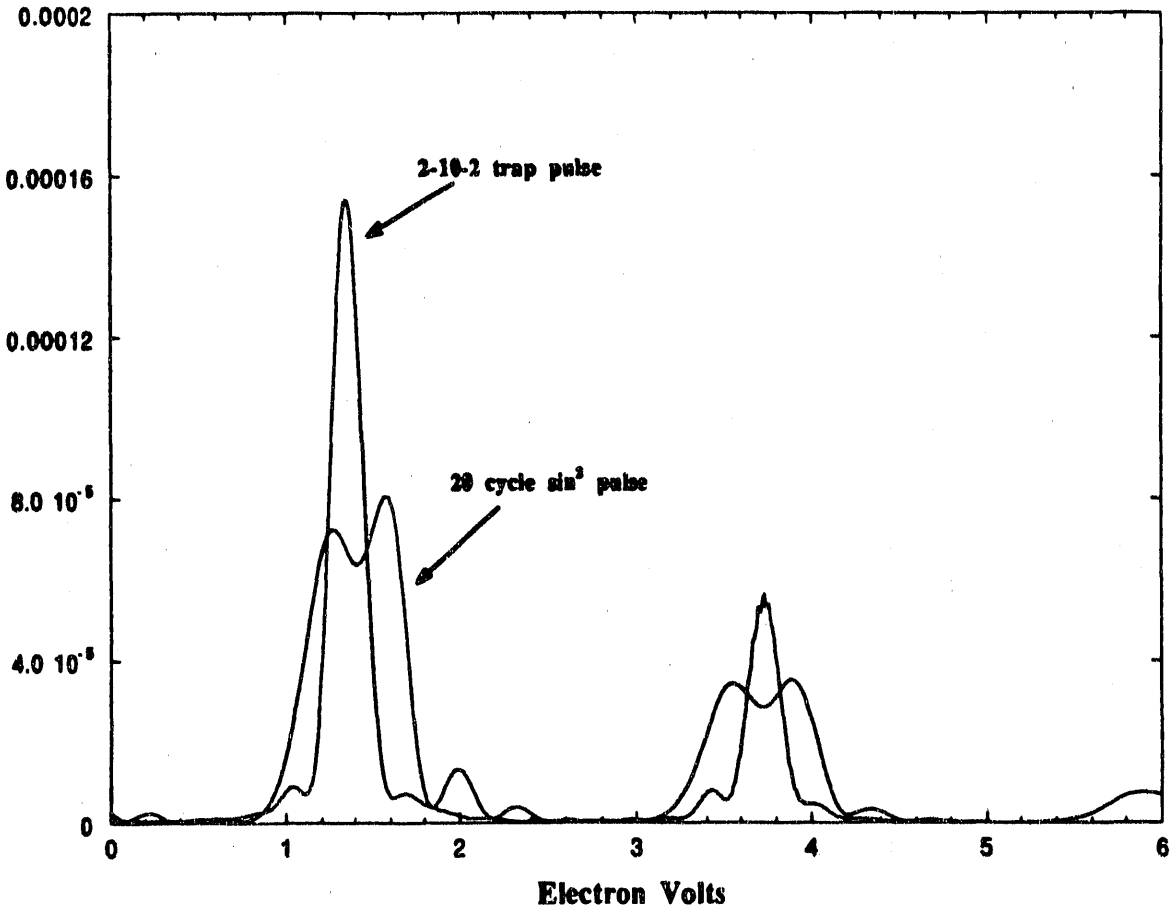

Figure 2-ATI spectra from a trapezoidal vs. $\sin^2$ pulse at 532 nm and 5×10^{13} W/cm^2.

fields will have both a magnitude and a phase relative to the driving field.[34] Second, the macroscopic harmonic fields due to the coherent emission from all the atoms are found by solving Maxwell's equations using as a source the single atom polarization fields. This second part accounts for the phase matching constraints due to the different indices of refraction for the harmonic and pump fields in the medium. This phase matching contribution to the overall emitted signal can be very important and will depend on the focal parameters of the laser, the density, the extent of ionization and the length of the active medium. Further details of the methods for solving this part of the problem are discussed in another paper in this volume.[35]

The calculation of the single atom emission spectrum can be accomplished by determining the induced time-dependent dipole of the laser excited atom.[18] This is simply the expectation value of the electronic coordinate along the axis of polarization:

$$d(t) = e \langle\psi(t) \mid z \mid \psi(t)\rangle. \tag{10}$$

The square of the Fourier transform of this dipole is proportional to the single atom emission spectrum.

At high intensities, the spectrum of harmonic intensities develops a plateau of approximately constant emission rates. Generally, the plateau follows a rapid decrease of intensity for the first few harmonics and is itself followed by an abrupt cutoff. This observed spectrum, of course, includes the effects of phase matching. However, it has been found that the single atom spectra, for almost any form of potential, one- to three-dimensional, short- or long-range, all exhibit this overall structure.[36-38] Thus, in the non-perturbative regime, the importance of phase matching is considerably reduced compared to the weak field case.[39] This conclusion is dependent on the laser being weakly focused such that its confocal parameter is larger than the propagation distance through the medium.

We have obtained single-atom harmonic spectra for several atoms, for the hydrogen molecule and for a model short-range (but three-dimensional) potential.[38] In figure 3 we show a representative result for neon, in a laser field with peak intensity of 1×10^{14} W/cm^2 at

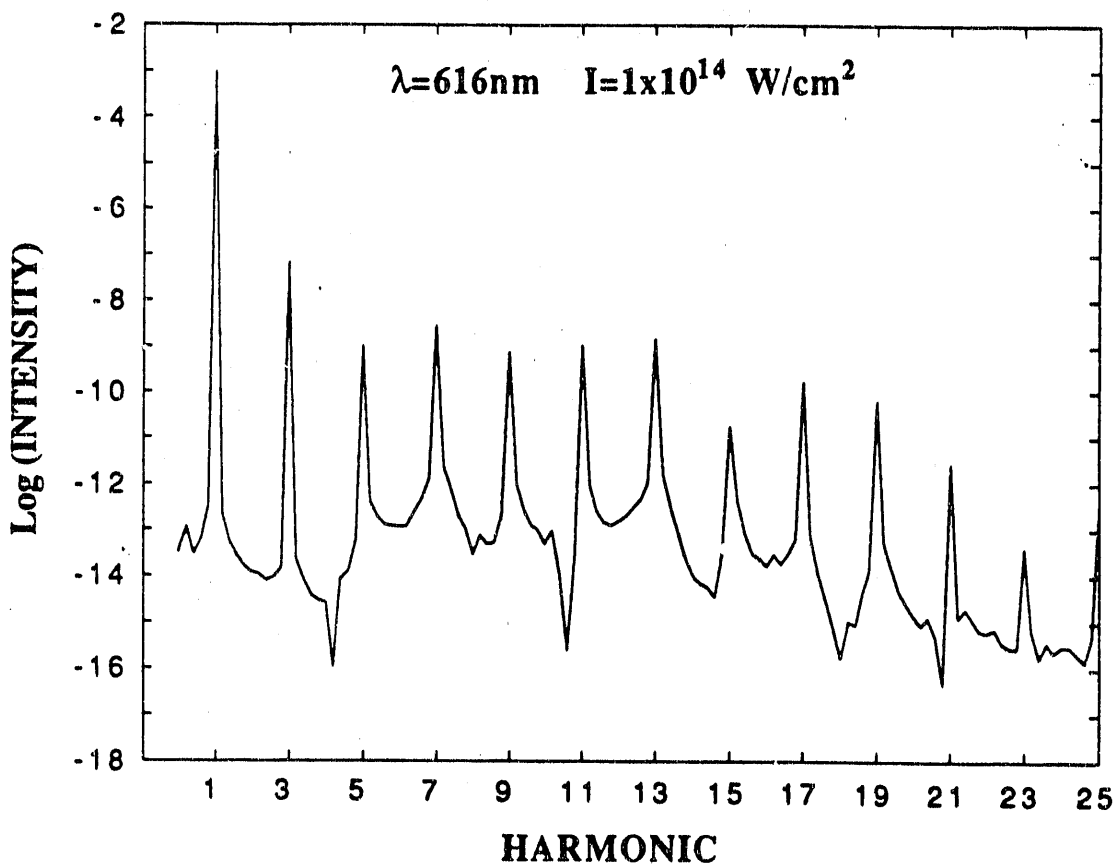

Figure 3-Neon single-atom photoemission spectrum.

a wavelength of 616 nm. The pronounced peaks, which are at the odd harmonics of the driving frequency lie, on a broad background. The width of the peaks correspond to the inverse of the pulse width or the ionization rate, whichever is less. The neon calculations are performed for a single outer shell electron moving in the field of the other atomic electrons,

held frozen in their ground state orbitals. The effective potential this electron sees has been generated from Hartree-Slater calculations on the ground and excited states of the system. These calculations utilized ℓ-dependent pseudopotentials which are superior to those used previously in our cylindrical coordinates code.[40] The p(ℓ=1) potential comes from the ground state of the system and the s(ℓ=0) potential from calculations on the $2p^5 3s$ excited state. In these calculations we have adjusted the Slater (Xα) parameter to insure that the ground and excited states have excitation energies as accurate as is possible within this single-electron model. Using these techniques we have found quantitative agreement, once the phase matching calculations have been carried out, with experimental conversion efficiencies for a number of atoms.[39]

In order to better understand the source of harmonic production, we studied several systems with widely varying potentials to see their effects on the single-atom emission spectrum. The results are illustrated in figure 4 in which we present harmonic spectra from the hydrogen atom, from the hydrogen molecule and from a short-range Yukawa potential all of which have have the same ionization potential. It has been found the the number of

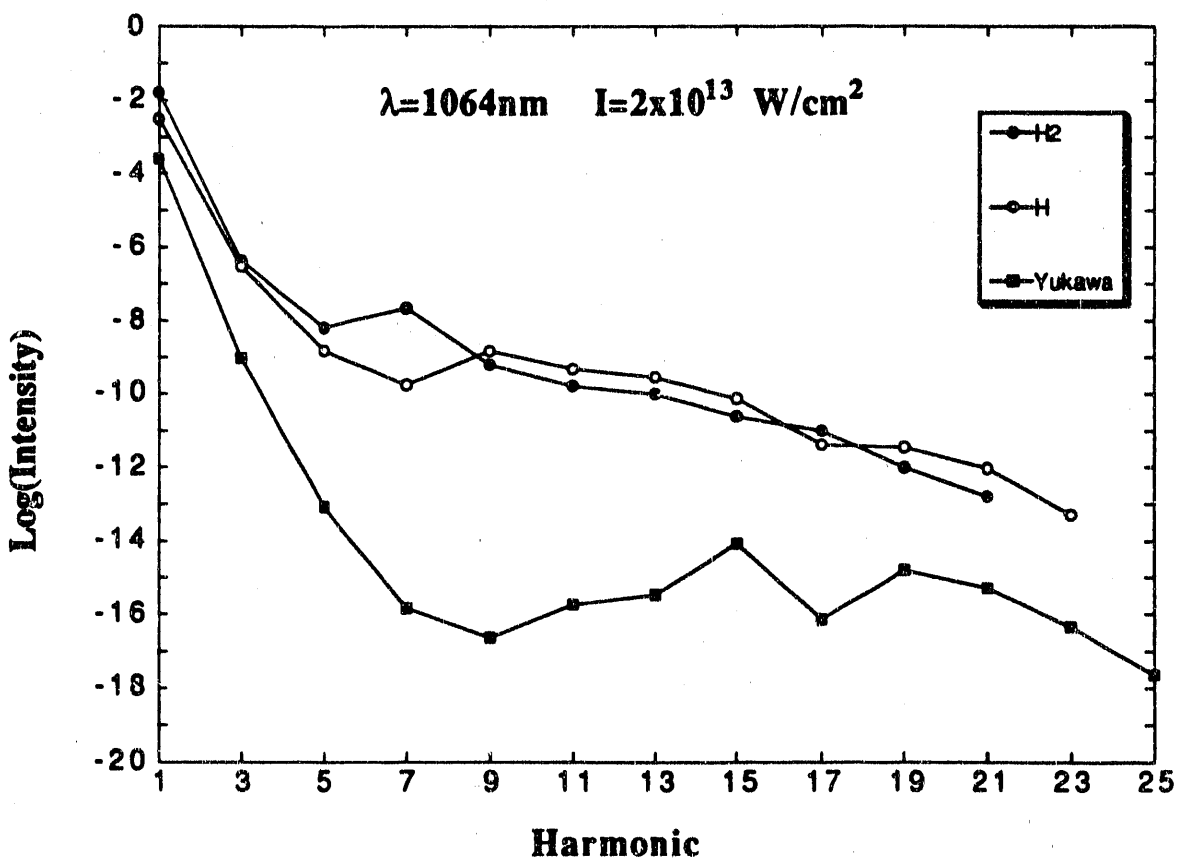

Figure 4-Single-atom harmonic intensities for the hydrogen atom, hydrogen molecule and a short range, Yukawa potential.

harmonics obtained for a given wavelength and laser intensity depends strongly on the ionization potential. The Yukawa potential has only one bound state. The H_2 molecule was

stretched from its equilibrium bond distance to 2.04 a_0 to give the desired ionization potential. Its bond length was held fixed during the calculation and the axis was oriented along the direction of polarization. The effective potential for the active electron in the H_2 model was obtained from a Hartree-Fock calculation in the manner previously employed for helium.[41]

As can be seen from figure 4, the emission from H and H_2 are in quite good agreement both in magnitude and in the number of plateau harmonics. The emission from the Yukawa potential is orders of magnitude less intense, but shows a plateau of comparable width to the other systems. The short-range parts of these three potentials are very similar for the Yukawa and the H-atom, but very different for H_2. Thus, it seems the short-range behavior of the potential is not terribly crucial to harmonic emission. The H and H_2 potentials are identical at long range, both supporting a Rydberg series converging to the ionization potential. It is these excited states which affect the conversion efficiency. By softening the Yukawa potential to introduce additional states in the well while keeping the ionization potential constant, we found its spectrum converged to the Coulomb results by the time four excited states were present. Thus, an entire Rydberg series is not necessary to obtain the higher results shown in this figure.

The background found in the calculated emission spectra may appear similar to that observed experimentally.[29] However, we found that, in contrast to the harmonic emission, the background emission carries no constant phase relative to the driving field and therefore the phase matching of this background will not occur. We expect this emission to be orders of magnitude weaker than the harmonic peaks so that our calculated background is unlikely to be responsible for that observed. Other mechanisms must contribute to the experimentally observed result.

TRAPPING/LOCALIZATION

Over the past several years, Gavrila and coworkers[42] have performed an interesting series of studies on the behavior of atoms in high frequency fields. They found that for photon energies which exceed the ionization potential of the system, raising the intensity high enough can cause stabilization of the atom. That is, as the intensity increases the ionization rate decreases. In fact, they have predicted that the ground state wave function actually bifurcates, having two maxima at the two turning points of the orbit of a classical electron, oscillating in the laser field in the absence of the potential. These turning points are given in terms of the field strength and frequency by (in atomic units)

$$\alpha = E/\omega^2. \tag{11}$$

These results are relevant to cases with $\alpha >> 1$. Because these calculations were time independent, they did not address the effects of the turn on of such a strong, high frequency laser. The question remained whether the atom could survive to be trapped in this unusual state.

Recently, Su, et al. used their one-dimensional soft Coulomb model to determine the survivability of the atom in a time-dependent high frequency field.[43] Their results clearly demonstrated that in this 1d case, the electronic state does become stabilized. The frequency chosen, however, corresponded to 2-photon ionization, so the assumptions made by Gavrila of high frequency may not have been valid. This was encouraging from an experimental point of view because it is possible to find strong, short pulse lasers which can cause 2-photon ionization of many atomic systems. Additionally, Su, et al. did observe their wave function having the bimodal structure predicted by Gavrila.

We have repeated the calculations of Su, et al. and find excellent agreement with their results. However, for some wavelengths and intensities the wave function is found to have a much more complicated structure than the two-peaked structure of Gavrila and Su. Once trapped, the structure remained stable in shape and oscillated in phase with the field over a range of approximately 2α.

These results encouraged us to pursue these calculations for a real three-dimensional atom. We consider a hydrogen atom in a field with a frequency of 1 a.u. (27.21 eV) which is twice its ionization potential. We present results for the following intensities 4, 16 and 64×10^{17} W/cm^2, corresponding to α of 3.4, 6.8 and 13.5, respectively. We used pulses which rose linearly over five optical cycles, then the intensity was held constant over the next ten cycles. Toward the end of these pulses we observed an exponential decay of the orbital which is due to absorbing boundaries on our grid which are well removed from the nucleus. (The distance to the boundary was much larger than α.) We believe the flux reaching the boundary is truly ionized since no mechanism exists to allow it to return to the vicinity of the atom. The probability remaining near the atom at the end of these pulses was 0.082, 0.310 and 0.515 for the three cases described above, respectively, and the calculated decay rates were 1.1×10^{15}, 2.7×10^{14} and $1\ 1 \times 10^{14}$ 1/s. These results definitely corroborate the earlier predictions, establishing that the 1d results carry over into the real world.

We find, however, that the trapped wave function again did not exhibit the predicted, bimodal structure. We show in figure 5 eight snap-shots of the evolving wave function during the 16th optical cycle for the 1.6×10^{18} W/cm^2 case. In general, we observe that some structure is excited during the turn on which, when it stabilizes, oscillates in the vicinity of the nucleus with an amplitude approximately equal to $\pm\alpha$. This oscillatory motion may not be centered on the nucleus as predicted by the Gavrila model. Also we found that as in the 1d calculations, if no intensity ramp is used in the pulse, no stabilization is found.

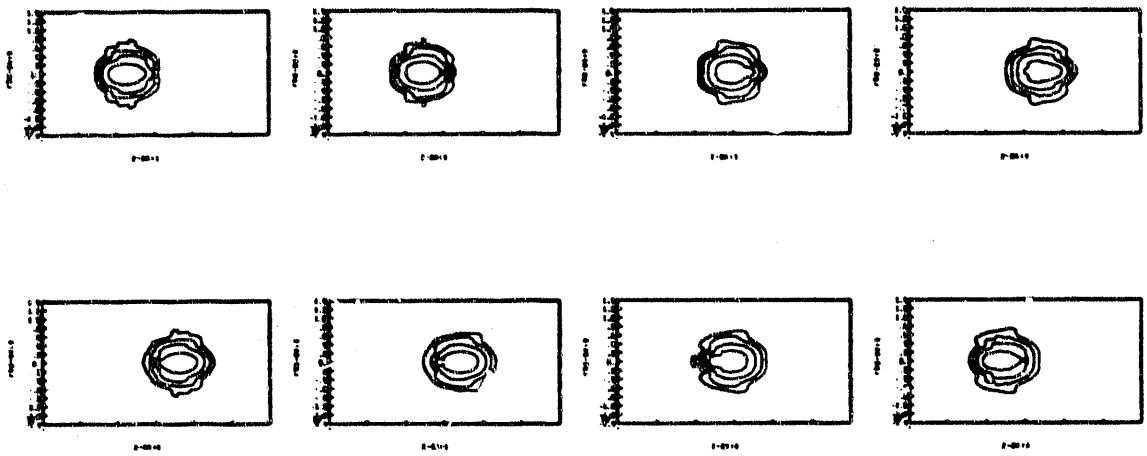

Figure 5-Snapshots of the electron density of a trapped hydrogen wave function during a single optical cycle. Tick marks along bottom axis are separated by 10 a_0; time increases left-to-right and top-to-bottom in increments of 1/8 cycle. Photon energy is 27.21 eV, the intensity is 1.6×10^{18} W/cm^2 corresponding to $\alpha = 6.8\ a_0$.

This work was performed under the auspices of the U.S. Department of Energy at Lawrence Livermore National Laboratory under contract number W-7405-Eng-48.

REFERENCES

1. For a recent review see S. I. Chu, Adv. *Chem. Phys.* 73, 739 (1989)
2. J. H. Eberly, J. Javanainen and K. Rzazewski, *Physics Reports* (in press)
3. K. C. Kulander, *Phys. Rev. A* 35, 445 (1987)
4. K. J. Schafer and K. C. Kulander, *Phys. Rev A* (in press)
5. K. C. Kulander and T. N. Rescigno, *Comp. Phys. Comm.* (in press)
6. K. J. Schafer, *Comp. Phys. Comm.* (in press)
7. R. S Varga, Matrix Iterative Analysis (Prentice Hall, Englewood Cliffs, N.J., 1962)
8. M. Hermann and J. A. Fleck, *Phys. Rev. A* 38, 6000 (1988)
9. P. L. DeVries, *J. Opt. Soc. Am. B* 7, 517 (1990)
10. K. J. LaGattuta, *J. Opt. Soc. Am. B* 7, 639 (1990)
11. K. J. LaGattuta, *Phys. Rev. A* 41, 5110 (1990)
12. M. S. Pindzola and C. Bottcher, *J. Opt. Soc. Am. B* 4, 752 (1987)
13. M. S. Pindzola, G. Bottrell and C. Bottcher, *J. Opt. Soc. Am. B* 7, 659 (1990)
14. X. Tang, H. Rudolph and P. Lambropoulos, submitted
15. J. K. Liakos and M. Horbatsch, *J. Opt. Soc. Am. B* 7, 685 (1990)
16. L. A. Collins and A. L. Mertz, *J. Opt. Soc. Am. B* 7, 647 (1990)
17. F.H.M. Faisal and J. V. Moloney, *J. Phys. B* 14, 3603 (1981)
18. K. C. Kulander and B. W. Shore, *Phys. Rev. Lett.* 62, 624 (1989)

19. S. I. Chen and J. Cooper, *Phys. Rev. A* 32, 2769 (1985)
20. M. Crance, *J. Phys. B* 21, 2697 (1988)
21. R. M. Potvliege and R. Shakeshaft, *Phys. Rev. A* 40, 3061 (1989)
22. R. M. Potvliege and R. Shakeshaft, *Phys. Rev. A* 41, 1609 (1990)
23. See, for example, A. Szöke, *J. Phys. B* 18, L427 (1985)
24. R. R. Freeman, P. H. Bucksbaum, H. Milchberg, S. Darack, D. Schumacher and M. E. Geusic, *Phys. Rev. Lett.* 59, 1092 (1987)
25. P. Agostini, P. Breger, A L'Huillier, H. G. Muller, G. Petit, A. Antonetti and A. Migus, *Phys. Rev. Lett.* 63, 2208 (1989)
26. M. D. Perry, A. Szöke and K. C. Kulander, *Phys. Rev. Lett.* 63, 1058 (1989)
27. H. Rottke, B. Wolff, M. Brickwedde, D. Feldmann and K. Welge, *Phys. Rev. Lett.* 64, 404 (1990)
28. A. McPherson, G. Gibson, H. Jara, U. Johann, T. S. Luk, I. A. McIntyre, K. Boyer and C. K. Rhodes, *J. Opt. Soc. Am. B* 4, 595 (1987)
29. M. Ferray, A. L'Huillier, X. Li, L. A. Lompré, G. Mainfray and C. Manus, *J. Phys. B* 21, L-31 (1988)
30. X. F. Li, A. L'Huillier, M. Ferray, L. A. Lompré and G. Mainfray, *Phys. Rev. A* 39, 5751 (1989)
31. J. F. Reintjes, Nonlinear Optical Parametric Processes in Liquids and Gases (Academic Press, Orlando, 1984)
32. B. W. Shore and K. C. Kulander, J. *Mod. Opt.* 36, 857 (1989)
33. A. L'Huillier, X. F. Li and L. A. Lompré, *J. Opt. Soc. Am. B* 7, 527 (1990)
34. K. C. Kulander and B. W. Shore, *J. Opt. Soc. Am. B* 7, 502 (1990)
35. A. L'Huillier, L. A. Lompré, G. Mainfray and C. Manus, this volume
36. J. H. Eberly, Q Su, J. Javanainen, *Phys. Rev. Lett.* 62, 881 (1989)
37. B. Sundaram and P. Milonni, *Phys. Rev. A* 41, 6571 (1990)
38. J. L. Krause, K. J. Schafer and K. C. Kulander, submitted
39. A. L'Huillier, K. J. Schafer and K. C. Kulander, submitted
40. K. C. Kulander, *Phys. Rev. A* 38, 778 (1988)
41. K. C. Kulander, *Phys. Rev. A* 36, 272[illegible] (1987)
42. See M. Pont, N. R. Walet and M. Gavrila, *Phys. Rev. A* 41, 477 (1990) and references therein
43. Q. Su, J. H. Eberly and J. Javanainen, *Phys. Rev. Lett.* 64, 862 (1990)

END

DATE FILMED

02 / 06 / 91